

Stationary spots and stationary arcs induced by advection in a one-activator, two-inhibitor reactive system

Igal Berenstein, Domenico Bullara, and Yannick De Decker

Citation: *Chaos: An Interdisciplinary Journal of Nonlinear Science* **24**, 033129 (2014); doi: 10.1063/1.4894826

View online: <http://dx.doi.org/10.1063/1.4894826>

View Table of Contents: <http://scitation.aip.org/content/aip/journal/chaos/24/3?ver=pdfcov>

Published by the [AIP Publishing](#)

Articles you may be interested in

[Adaptive two-regime method: Application to front propagation](#)

J. Chem. Phys. **140**, 124109 (2014); 10.1063/1.4868652

[Bifurcation characteristics of fractional reaction-diffusion systems](#)

AIP Conf. Proc. **1493**, 290 (2012); 10.1063/1.4765503

[Design and control of patterns in reaction-diffusion systems](#)

Chaos **18**, 026107 (2008); 10.1063/1.2900555

[Concentration fluctuations in nonisothermal reaction-diffusion systems](#)

J. Chem. Phys. **127**, 034501 (2007); 10.1063/1.2746326

[Pursuit-evasion predator-prey waves in two spatial dimensions](#)

Chaos **14**, 988 (2004); 10.1063/1.1793751



computing
IN SCIENCE & ENGINEERING

AIP's JOURNAL OF COMPUTATIONAL TOOLS AND METHODS.
AVAILABLE AT MOST LIBRARIES.

Stationary spots and stationary arcs induced by advection in a one-activator, two-inhibitor reactive system

Igal Berenstein, Domenico Bullara, and Yannick De Decker

Center for Nonlinear Phenomena and Complex Systems (CENOLI), NonLinear Physical Chemistry Unit, Université libre de Bruxelles (ULB), Campus Plaine, C.P. 231, Brussels B-1050, Belgium

(Received 18 June 2014; accepted 26 August 2014; published online 4 September 2014)

This paper studies the spatiotemporal dynamics of a reaction-diffusion-advection system corresponding to an extension of the Oregonator model, which includes two inhibitors instead of one. We show that when the reaction-diffusion, two-dimensional problem displays stationary patterns the addition of a plug flow can induce the emergence of new types of stationary structures. These patterns take the form of spots or arcs, the size and the spacing of which can be controlled by the flow. © 2014 AIP Publishing LLC. [<http://dx.doi.org/10.1063/1.4894826>]

Turing patterns are known to occur in two-dimensional domains either as spots, as stripes or a mixture of the two. Other types of stationary patterns can be obtained with flow-distributed oscillations, in which an advective flow translates an oscillation in time into spatial dynamics. These flow-distributed oscillations are known to generate, in two dimensions, stripes that are parallel to the feeding boundary. Here, we present a system in which different stationary patterns, such as spots or arcs, can be obtained when advection is included. We also assess the extent to which the spatial frequency of such structures can be tuned by the advective flow.

This property makes advection a promising candidate for the control of spatial structures “on demand.” Its applicability should however be tested in the more realistic case of two-dimensional systems, which are known to often present qualitatively different behaviors as compared to their one-dimensional counterpart. In particular, there is no report as of today about the possibility to create and control two-dimensional stationary structures, such as spots, by adding advection to a reaction-diffusion system. The purpose of this paper is to show, thanks to numerical simulations, that such two-dimensional, advection-controlled pattern formation is feasible.

In Section II, we discuss the general conditions under which steady structures are formed for systems described by reaction-diffusion (RD), and by reaction-diffusion-advection (RDA) equations. A special emphasis is put on how the addition of a flow modifies the original RD picture. Section III is devoted to a presentation of the model we will use, which is an extension of the two-variable “Oregonator” that was originally developed for the Belousov-Zhabotinsky reaction.⁷ The results of numerical investigations presented in Sections IV and V form the main body of this work. We analyze the different dynamical regimes of the model and we assess the efficiency of advection-based structural control. We finally discuss in Section VI the relevance of these results in the context of the theory of pattern formation.

I. INTRODUCTION

The last few decades have witnessed an ever-growing interest for the use of non-equilibrium reactive processes in the synthesis of materials with well-defined, controllable spatial structures.^{1–3} The rationale for this approach is that some systems involving the reaction and the diffusion of molecules can sustain stationary patterns, when kept far away from equilibrium. In principle, the morphological properties of such structures can be controlled via external parameters or a clever design of the geometry of the reactor. In practice, however, such control strategies can sometimes reveal cumbersome. It is relatively easy to vary some of the external parameters, like the temperature or chemical feeds, to induce changes in the observed structures. An actual control of the spatial properties of the patterns on the other hand typically requires spatiotemporal variations of the control parameters, the implementation of which is often complex. In such cases, alternative control strategies need to be used such as the illumination of photosensitive systems.

Another route to the synthesis and control of spatial structures has been proposed recently.^{4–6} Advective flows were shown to produce stationary patterns in a theoretical model for a one-dimensional reactive system, which in the absence of advection would give birth to propagating waves.⁶ Remarkably, the wavelength and the shape of these steady patterns can be adjusted by the intensity of the flow.

II. STATIONARY SPATIAL STRUCTURES IN REACTION-DIFFUSION-ADVECTION SYSTEMS

In reaction-diffusion systems stationary spatially periodic patterns are obtained with activator-inhibitor dynamics, when the inhibitor diffuses faster than the activator as described by Turing.⁸ These patterns in two-dimensional domains typically exist as spots or stripes, or as a mixture of the two.^{9,10}

Advective flows are also known to induce both stationary and moving spatially periodic patterns, when the local dynamics is itself periodic in time. This phenomenon is known as flow distributed oscillations (FDOs).^{4,5,11} In two-dimensional domains, however, these FDOs only appear as

stripes that are parallel to the boundary where the flow comes from or, equivalently, to a moving boundary.¹²⁻¹⁵ One could think that having a Turing instability in a reaction-diffusion system helps to obtain stationary spots in the corresponding RDA case. However, it was shown that this instability is an obstacle to the formation of stationary structures in RDA systems: In such cases, one usually observes Turing patterns drifting with the flow. Temporal oscillations are needed on top of the Turing instability to obtain stationary patterns.¹⁶ The structures obtained in such a way thus have the same properties as the FDOs, and consequently, a pattern of stationary spots or arcs cannot be obtained.

More recently, it was found that a RDA system with wave instability produces stationary patterns in one dimension, at low velocities of the flow.^{6,17} In order to test if such a mechanism can sustain a pattern of stationary spots, we study here the same three-variable system as in Ref. 6, but in two dimensions.

III. THE MODEL

The model we use consists in the following set of partial differential equations:

$$\frac{\partial x}{\partial t} + \mathbf{v} \cdot \nabla x = \frac{1}{\varepsilon} \left[x(1-x) - f_y \left(\frac{x-q_y}{x+q_y} \right) - f_z \left(\frac{x-q_z}{x+q_z} \right) \right] + D_x \nabla^2 x, \tag{1}$$

$$\frac{\partial y}{\partial t} + \mathbf{v} \cdot \nabla y = a(x-y) + D_y \nabla^2 y, \tag{2}$$

$$\frac{\partial z}{\partial t} + \mathbf{v} \cdot \nabla z = \kappa x - (1-a)z + D_z \nabla^2 z. \tag{3}$$

This system is a modification of the two-variable Oregonator model for the Belousov-Zhabotinsky reaction. It involves the two-dimensional concentration field of one activator (x) and of two inhibitors (y and z). The vector velocity field is set to be constant, with all the field arrows being parallel to one of the axes, *in extenso* $\mathbf{v} = (v_1, v_2) = (0, -v)$. This situation would correspond to a reactor operating in the plug flow mode, with the flow going downwards. The diffusion coefficients are chosen so that one of the inhibitors and the activator are diffusing slowly ($D_x = D_z = 0.1$), while the other inhibitor diffuses fast ($D_y = 2$). The parameters q_y and q_z are (as for the Oregonator model) ratios of kinetic constants. In the present study, we will always consider cases for which $q_y = q_z = q$. ε and κ are time separation parameters, while f_y and f_z control the extent of the inhibitory effects of y and z , respectively. The parameter a is always greater than 0 and smaller than 1. It tunes which reaction pathway is preferred: For $a = 1$, the inhibitor z would tend to accumulate. A more detailed description of this model can be found elsewhere.⁶

In the homogeneous limit, the model admits two physically relevant steady states. One of them is trivial, as it corresponds to an empty system ($x_s = y_s = z_s = 0$). A linear stability analysis of this state reveals that it is unstable (it is a saddle point) for all values of the parameters. The other steady state is given by

$$x_0 = y_0 = \left(\frac{1-a}{\kappa} \right) z_0 = \frac{1-q-A}{2} + \frac{1}{2} \sqrt{(1-q-A)^2 + 4q(1+A)} \tag{4}$$

with $A = f_y + f_z \kappa / (1-a)$. This state can be stable or unstable with respect to homogeneous perturbations, depending on the conditions. Consider, for example, the ensemble of steady states corresponding to $a = 3/4$, $\kappa = 0.16$, $\varepsilon = 0.04$, and $q = 0.01$ (we will keep the same values in our investigation of pattern formation). The corresponding state diagram, in the f_y - f_z parametric plane, is depicted in Figure 1.

For very large and very low values of both these control parameters, the state is a stable node or focus (grey zones in the diagram). For intermediate values, three types of instabilities can be observed, in zones marked as I, II, and III, respectively. Note that the boundaries between the zones of stability and both zones I and III correspond to a Hopf bifurcation. Starting at large values of f_z , and decreasing this parameter at constant f_y , the stable node thus first becomes a stable focus and under a given critical point f_z^H , it turns to a repeller because of the Hopf bifurcation. Numerical simulations confirm this analysis and show the existence of a limit cycle. However, they also reveal that the system undergoes a series of complex transitions, shortly after the Hopf bifurcation has been crossed. Mixed mode oscillations can be found (zone II in Figure 1), the amplitude and period of which change in a stepwise fashion as f_z is lowered. The properties of these complex, nonlinear behaviors cannot be assessed any more with linear stability analysis. For low enough values of f_z , one observes simple period-1 oscillations again (zone III in the diagram). All the behaviors of interest that we report in the remainder of this work were obtained for such values of the parameters. It should finally be noted that for low values of f_y , the oscillations eventually disappear through a Hopf bifurcation, and one has a single stable state again (grey zone on the bottom left in Figure 1).

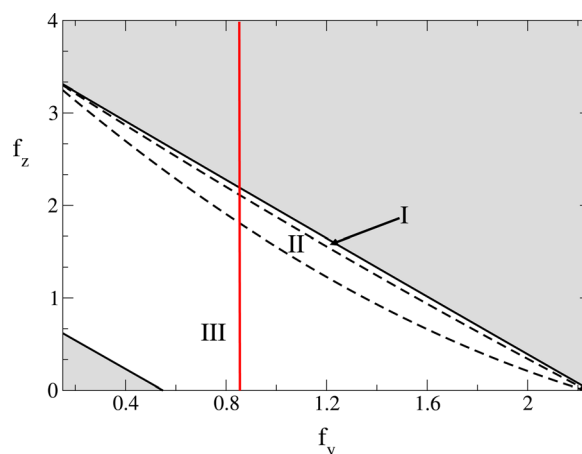


FIG. 1. State diagram of the homogeneous system for $a = 3/4$, $\kappa = 0.16$, $\varepsilon = 0.04$, and $q = 0.01$. They grey regions correspond to the zones of stability of the state of reference. In zones I and III, one has simple oscillations resulting from a Hopf bifurcation, while in zone II mixed-mode oscillations are observed (see text for more details). The vertical line represents the case $f_y = 0.85$.

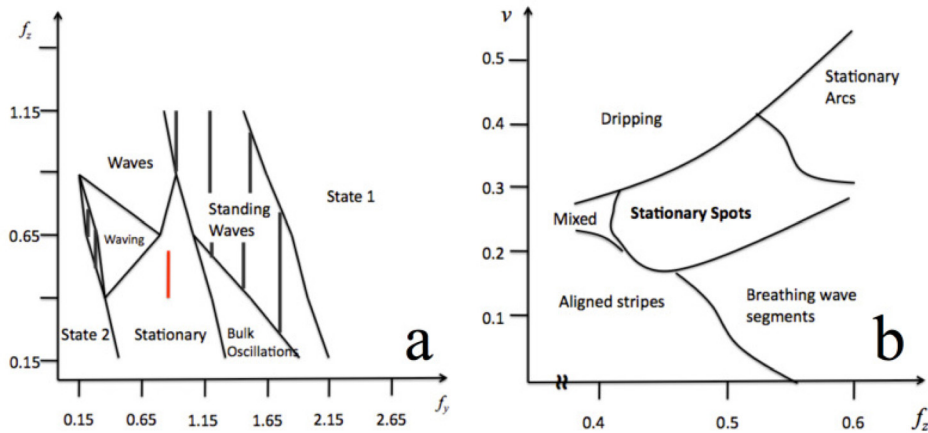


FIG. 2. (a) Phase diagram of patterns in the one-dimensional case, in the f_z - f_y plane. The red line highlights the region in which we performed the two-dimensional simulations. (b) Overview of two-dimensional patterns in the f_z - v domain, for $f_y = 0.85$. The values of the parameters and the boundary conditions are as mentioned in the text.

Before turning to the spatiotemporal dynamics of the full model, we will first discuss the reaction-diffusion (advection free) problem.

IV. PATTERN FORMATION IN THE ABSENCE OF ADVECTION

Previous numerical investigations showed that the above model leads to complex spatiotemporal behaviors, in the case of a reaction-diffusion, one-dimensional system.⁶ We observe similar behaviors in the two-dimensional case. We perform numerical integrations of the reaction-diffusion system, using both finite differences and finite element methods, with the set of parameters given above. The initial conditions always correspond to the non-trivial steady state, to which low amplitude random perturbations are added. We use as boundary conditions Dirichlet on top (with $x = y = z = 0.1$), and no flux at the bottom and on the sides of the two-dimensional systems, which corresponds to what is usually used for numerical studies for plug flow reactors.^{5,6,11,17} The different dynamical behaviors are summarized in Figure 2(a). To illustrate the complexity of the model, we consider the case $f_y = 0.85$ and vary f_z , starting from large values at which the steady state is spatially stable (as can be easily shown with spatially dependent linear stability analysis).

As predicted by the linear stability analysis, the system undergoes a homogeneous Hopf bifurcation at $f_z \approx 2.223$ and one observes an oscillatory dynamics. Because of our choice of boundary conditions, the oscillations start from the lower side of the system, and subsequently move up towards the boundary where Dirichlet conditions are maintained. After this transient, a spatially homogeneous periodic behavior is observed. The mixed mode oscillations observed for

lower values of f_z in the well-mixed case appear as standing waves, whose period is twice that of the original uniform oscillations. The same behavior was observed in one dimension as well.⁶ As f_z is decreased, travelling spots and then travelling waves are also seen (after the above mentioned transient). For lower values of this parameter, the observed dynamics changes qualitatively and seems to result from a competition between travelling patterns and a stationary periodic organization. The origin of the spatially periodic pattern is clear: The system undergoes a Turing bifurcation at $f_z \approx 1.847$, and the wavelength observed in numerical integrations is always close to the wavelength at which the eigenvalue of the linear problem presents a maximum. The complex dynamics that we observe thus bears similarities with the classical Turing-Hopf interaction, including spatiotemporal chaos.¹⁸

A detailed bifurcation analysis of the system is beyond the scope of the present work, in which we focus on behaviors observed only at low enough values of f_z . The well-mixed system then admits simple period-1 oscillations of large amplitude. When diffusion is included, we observe that the homogeneous oscillations are lost. One has instead either regular Turing patterns or spatiotemporal chaos (see Figures 2(b) and 3). The Turing structures usually consist in a mixture of spots and stripes, with the latter tending to align parallel to the upper side of the system (Figure 3(a)). The spatiotemporal chaotic behavior appears as breathing wave segments (see Figure 3(b)). This behavior is also seen in the presence of advection, and will be described in more detail in Section V.

It has been often reported in the literature that the addition of a flow typically results in an advection of the

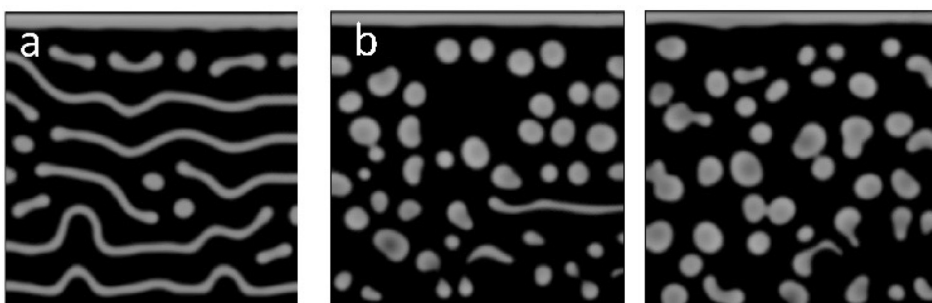


FIG. 3. Patterns at $v=0$ (a) stationary pattern obtained with $f_z = 0.4$ at 100 time units after starting the simulation and (b) spatiotemporal chaos with $f_z = 0.6$ at 50 and 100 time units, respectively. The values of the other parameters are given in the text.

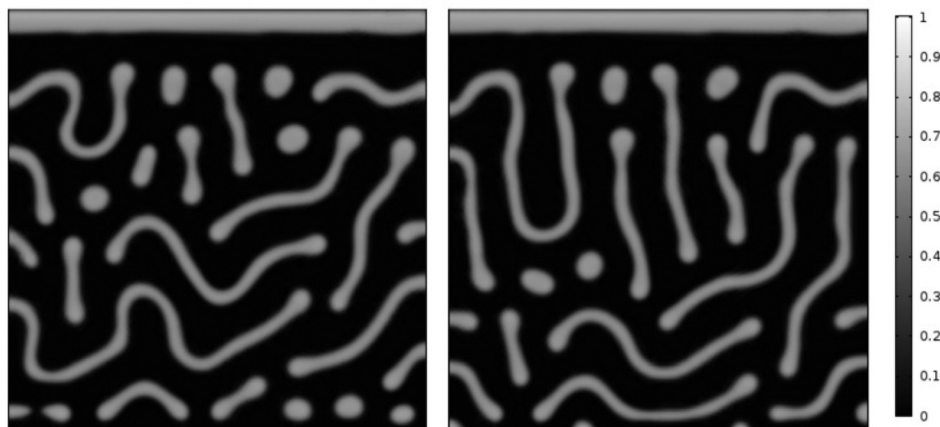


FIG. 4. Aligning stripes, obtained for $f_z = 0.4$ and $v = 0.1$. Pictures of the variable x (20 space units \times 20 space units) are taken at 50 (left) and 100 (left) time units, respectively. The color scale is presented on the right side of the picture.

corresponding reaction-diffusion patterns (see, for example, Ref. 16). We also observed such a trend, for most values of f_z . However, for low values of this parameter, we observe qualitatively new behaviors. We report and analyze them in Sec. V.

V. ADVECTION-INDUCED PATTERNS

In the remainder of this work, we focus on the parametric region depicted in red in Figure 2(a) (and thus again for $f_y = 0.85$), where we observe new types of spatiotemporal structures. An overview of these results is depicted in Figure 2(b), where in the absence of advection, the system presents either stationary patterns or spatiotemporal chaos.

As v is increased, we observe (as expected) that the reaction-diffusion patterns simply tend to get advected. The breathing wave segments travel downwards, and the Turing structures tend to align along the direction of the flow, in other words, perpendicular to the upper boundary where the Dirichlet condition holds. Also, the value of f_z marking the

transition between these two regimes is shifted towards lower values. For more rapid flows, however, the situation changes dramatically.

At sufficiently rapid flows and for low values of f_z , we see two regimes involving moving patterns. One of them corresponds to the coexistence of stationary and moving stripes aligning with the flow (in the “aligned stripes” region) (see Figure 4). Note that this behavior is strikingly different from the one-dimensional situation, for which it was observed that the system adopts a stationary structure for the same choice of parameters.⁶

The other regime consists in what we call “dripping patterns,” and is observed at large values of v only. An example of such phenomenon is given in Figure 5. As before, the dynamics starts with an oscillation located on the lower side of the system, which subsequently travels upwards as a band. The first oscillation creates in such a way a line that sticks to the top. The following ones move up but, instead of aligning with the flow like they do for small v , they break down into several arc-shaped fragments of similar size. These arcs

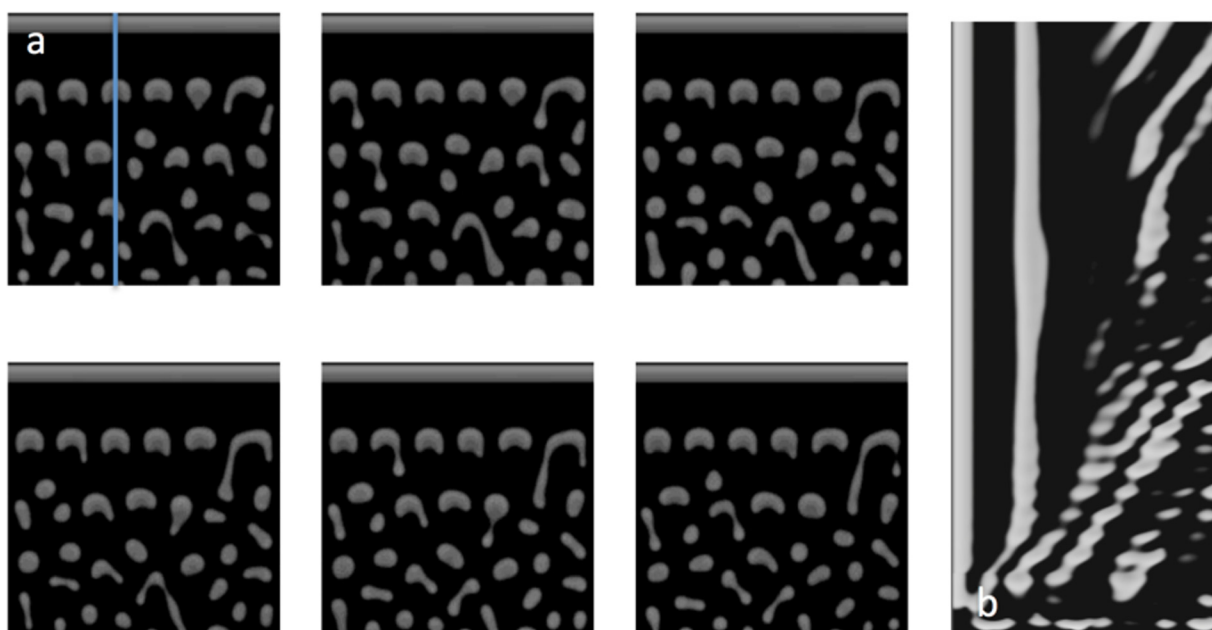


FIG. 5. Dripping patterns, obtained for $f_z = 0.4$ and $v = 0.4$. (a) Pictures of the variable x taken every 2 time units, starting at $t = 80$. (b) Space-time plot taken at the level of the line depicted in the first picture.

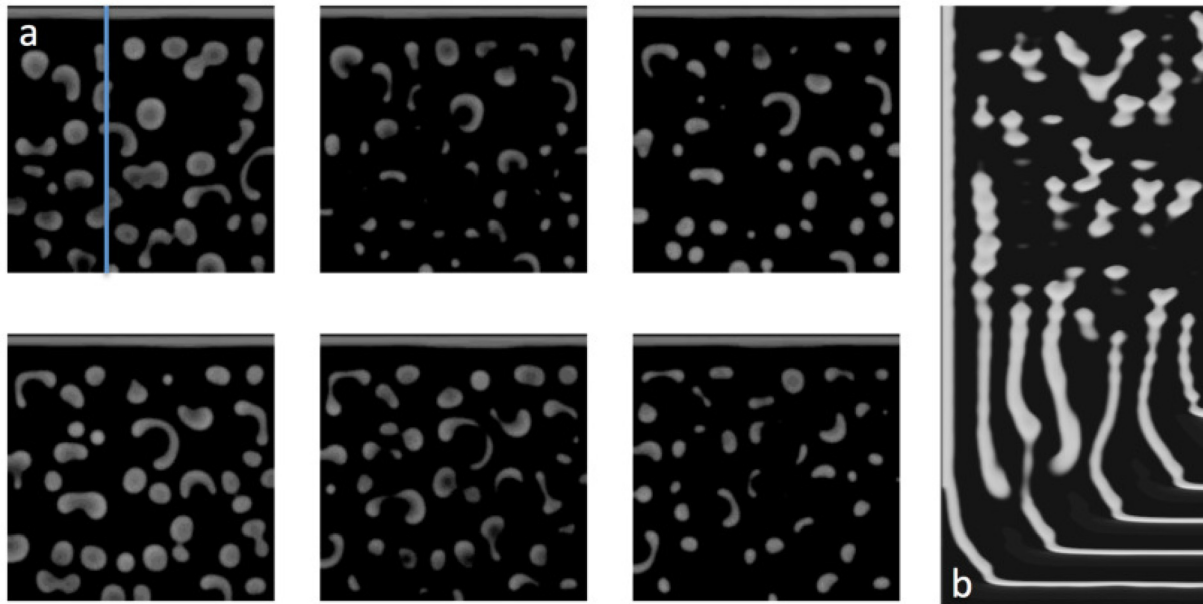


FIG. 6. Breathing wave segments, for $f_z = 0.6$ and $v = 0.1$. (a) Pictures of the variable x are taken every 1 time unit starting at $t = 95$. (b) Space-time plot taken at the line in the first picture.

accumulate at a well defined distance from the first band. From the tips of these arcs, which are stationary in space, a drop may develop and separate from the originating structure. As it separates it moves downwards with the flow forming a new stationary arc and displacing the structure that was there before. These drops thus generate a cascade of displacing patterns, as the structures that are displaced by a drop in turn displace the structures that are below them. As v is increased, the wavelength of the pattern in the direction of the flow increases. Similarly, the wavelength of the pattern perpendicular to the flow increases as well. The arcs become bigger and more bent for larger v , which leads to a decrease of the spatial frequency of that pattern.

For large values of f_z , breathing wave segments are again observed at moderate flows (see Figure 6). These patterns have two distinct phases. The breathing behavior is seen as the periodic rounding of the structures and seems somewhat reminiscent of breathing waves observed as interaction of traveling waves and oscillations inside a feeding chamber.¹⁹ The tips of the segments propagate rather than

curl up, as seen in regular reaction-diffusion waves. The propagation of the tips is important as it leads to the break-up of the structures.

More interestingly for our main purpose, new *stationary* structures can also be found for non-zero velocities of the flow. For large values of f_z and v , *stationary arcs* are observed. They correspond to the bent structures seen in the dripping case (see Figure 7), except that the dripping phenomenon is now only temporary. For long enough times, well defined arrays of immobile arcs are thus formed. The periodicity of the pattern can be tuned, to some extent, by changing the velocity of the flow. We indeed observe that it influences the periodicity of the pattern in the same way it does for the dripping arcs. Namely, the wavelength of the pattern in the vertical and the horizontal directions become larger when v increases. The period of the pattern along the flow generally increases faster than the one perpendicular to it.

For intermediate values of f_z and v , *stationary spots* are observed, as shown in Figure 8. It is worth noting that the stationary pattern with the same conditions but with no flow

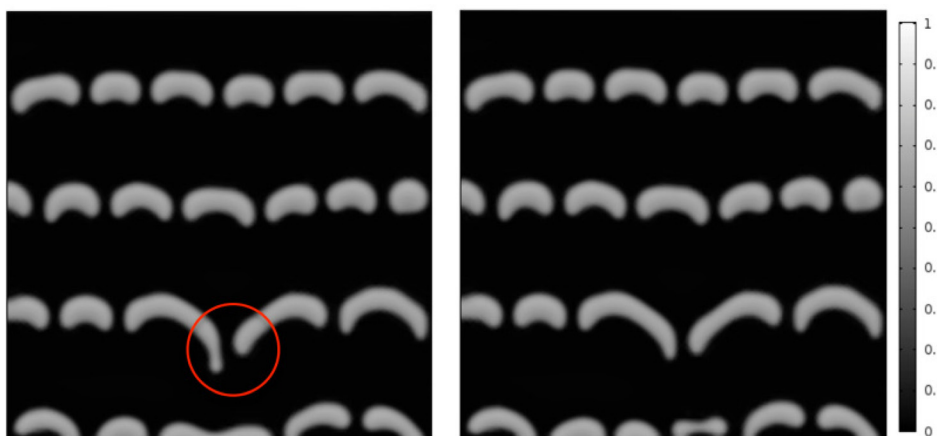


FIG. 7. Stationary arcs, obtained at $f_z = 0.6$ and $v = 0.5$. The pictures represent again the variable x and are taken $t = 200$ (left) and $t = 500$ (right). The region marked by the red circle shows some localized, temporary dripping as described in the text.

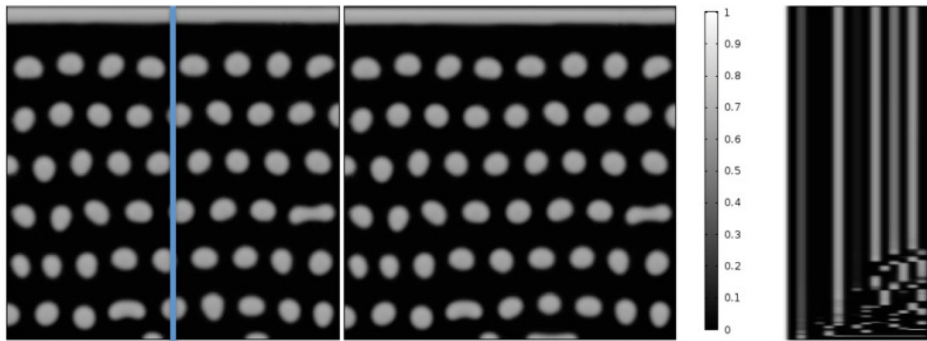


FIG. 8. Stationary spots, obtained at $f_z = 0.5$ and $v = 0.2$. The variable x is depicted at $t = 200$ (left) and $t = 500$ (center). A space-time plot is also depicted (right), and was taken at the line in first picture.

($v = 0$) corresponds to a mixture of spots and stripes. These spots appear, just like the arcs, because of the breaking down of bands emanating from the lower side of the system. In this case, though, the flow velocity is usually lower, and the fragments created in such a way are smaller and rounder. For long times, these spots arrange themselves according to a regular hexagonal pattern, the wavelength of which seems to be fixed by the choice of parameters, in the sense that it is barely affected by changes in the flow intensity. Finally, the “mixed pattern” region comprises systems in which aligned stripes, stationary spots, and dripping patterns coexist.

VI. CONCLUSIONS AND OUTLOOK

We have shown that it is possible to form a pattern of stationary spots or stationary arcs, in a particular case of reaction-diffusion-advection. The shape and periodicity of these patterns can be controlled, to some extent, by adjusting the intensity of the flow. In contrast to one-dimensional systems, at very low flow speeds, two-dimensional systems do not show a stationary pattern but a drifting one. The stripes that are generated by the system align with the flow, and defects in this pattern move accordingly. Stationary patterns at low flows are therefore more restricted in two-dimensional systems than in one dimension.

The question of the general conditions under which such patterns could appear naturally arises. First, it would seem that three variables are necessary for the sort of structures we observe here. The case of two-variable systems with differential diffusion has been treated earlier¹⁶ and no stationary spots could be observed in that case. Second, the ratio of diffusivities plays an important role. With equal diffusivities, the present model behaves in a way that is similar to what is seen for two-variable models.¹⁷ If both inhibitors diffuse fast, slow advection produces drifting patterns, while large advection can produce flow-distributed oscillation,¹⁷ but again no stationary spots or arcs are observed. The results we report here are thus only observed when one of the inhibitors, y , diffuses faster than the two other species. Finally, the intensity of the advective flow is an important parameter as well. For low values of v , the spatiotemporal dynamics is more or less that of the reaction-diffusion system, while for large v s the concentrations are simply advected away by the flow. The transversal symmetry breaking leading to spots is observed for intermediate flow velocities, where transport by diffusion and advection become comparable.

One could thus expect spots or arcs to form in other similar three-variable models respecting the above constraints on the diffusivities and flow velocity. However, these conclusions are based at this stage solely on a comparison of different numerical investigations of specific systems. The model we have used is tunable, in the sense that one of the parameters (a) permits to choose the pathway through the fast or slowly diffusing inhibitors. We have chosen a value of this parameter such that the area of stationary patterns in the parametric domain is large.⁶ The parameter range where stationary structures appear may be reduced or absent altogether in other cases, because of the specificities of the model at hand. It would be highly desirable to study the appearance of spots and arcs in a more generic fashion, preferentially on a simpler model so as to be able to extract analytical conditions for their emergence. A connection could be established in this way between the patterns we observe and dividing blobs and splitting spots or jumping waves observed in some reaction-diffusion systems.^{20,21}

The results presented here also lead to the question of the role played by advection in the emergence of stationary patterns in biological systems. The Turing instability is rather general and it has proven to be of importance in biology where, alongside a growing domain, it can predict the patterning of fish skin.²² Also, stationary patterns arising from an oscillatory behavior in a growing system forms a general mechanism that has a biological counterpart, like, for instance, the expression of genes during somitogenesis.¹⁴ The mechanism we presented here involves specific kinetics (simple and mixed mode oscillations, together with a Turing bifurcation) and takes place in a restricted interval of flow velocities and parameters. We therefore think that it is not a very likely candidate for pattern formation in biology.

However, the ability to produce systems with varying chemical concentrations (spatial control) is of great interest in chemistry, developmental biology, and for the design of emergent structures and phenomena, to cite but a few.²³ Microfluidic devices have become a common tool for these fields. Since the flow in such systems is laminar, the flow-induced path to producing stationary patterns could be observed and reveal useful, in particular for systems involving activator-inhibitor dynamics.

ACKNOWLEDGMENTS

I.B. thanks the Bureau des Relations Internationales et de la Coopération of the ULB, for financial support.

- ¹B. A. Grzybowski, K. J. M. Bishop, C. J. Campbell, M. Fialkowski, and S. K. Smoukov, *Soft Matter* **1**(2), 114–128 (2005).
- ²S. Mann, *Nat. Mater.* **8**(10), 781–792 (2009).
- ³A. S. Mikhailov and G. Ertl, *Chem Phys Chem* **10**, 86–100 (2009).
- ⁴M. Kaern and M. Menzinger, *Phys. Rev. E* **60**, R3471 (1999).
- ⁵P. Andresén, M. Bache, E. Mosekilde, G. Dewel, and P. Borckmans, *Phys. Rev. E* **60**, 297–301 (1999).
- ⁶I. Berenstein, *Chaos* **22**, 023112 (2012).
- ⁷J. J. Tyson, *J. Phys. Chem.* **86**, 3006–3012 (1982).
- ⁸A. M. Turing, *Philos. Trans. R. Soc. London, Ser. B* **237**, 37–72 (1952).
- ⁹Q. Ouyang and H. L. Swinney, *Nature* **352**, 610–612 (1991).
- ¹⁰B. Rudovics, E. Barillot, P. W. Davies, E. Dulos, J. Boissonade, and P. De Kepper, *J. Phys. Chem. A* **103**, 1790–1800 (1999).
- ¹¹J. R. Bamforth, J. H. Merkin, S. K. Scott, R. Tóth, and V. Gáspár, *Phys. Chem. Chem. Phys.* **3**, 1435–1438 (2001); J. R. Bamforth, R. Tóth, V. Gáspár, and S. K. Scott, *ibid.* **4**, 1299–1306 (2002); J. R. Bamforth, S. Kalliadasis, J. H. Merkin, and S. K. Scott, *ibid.* **2**, 4013 (2000).
- ¹²D. G. Míguez, G. G. Izús, and A. P. Muñuzuri, *Phys. Rev. E* **73**, 016207 (2006).
- ¹³M. Kaern, R. Satoianu, A. P. Muñuzuri, and M. Menzinger, *Phys. Chem. Chem. Phys.* **4**, 1315–1319 (2002).
- ¹⁴M. Kaern, M. Menzinger, and A. Hunding, *Biophys. Chem.* **87**, 121–126 (2000).
- ¹⁵D. G. Míguez, R. A. Satoianu, and A. P. Muñuzuri, *Phys. Rev. E* **73**, 025201(R) (2006).
- ¹⁶A. Yochelis and M. Steintuch, *Phys. Chem. Chem. Phys.* **12**, 3957–3960 (2010).
- ¹⁷I. Berenstein, *Chaos* **22**, 043109 (2012).
- ¹⁸A. De Wit, G. Dewel, and P. Borckmans, *Phys. Rev. E* **48**, R4191 (1993).
- ¹⁹I. Berenstein, A. P. Muñuzuri, L. Yang, M. Dolnik, A. M. Zhabotinsky, and I. R. Epstein, *Phys. Rev. E* **78**, 025101(R) (2008).
- ²⁰P. W. Davies, P. Blanchedeau, E. Dulos, and P. De Kepper, *J. Phys. Chem. A* **102**, 8236–8244 (1998).
- ²¹A. A. Cherkashin, V. K. Vanag, and I. R. Epstein, *J. Chem. Phys.* **128**, 204508 (2008).
- ²²S. Kondo and R. Asai, *Nature* **376**, 765–768 (1995).
- ²³Y. V. Kalinin, A. Murali, and D. H. Gracias, *RSC Adv.* **2**, 9707–9726 (2012).